Proceedings of the 11th World Congress on Electrical Engineering and Computer Systems and Sciences (EECSS'25)
Paris, France - August, 2025
Paper No. EEE 105
DOI: 10.11159/eee25.105

Development Octagonal in Concentric and Meander Line Slot Antennas for Optimal RFID Performance for Safety Food

Cheima Ben Hattab[1]
[1]University of Salento
Via Lecce-Monteroni, 73047 Monteroni di Lecce LE, Italy
Cheima.Benhattab@unisalento.it

Abstract **-** RFID technology, first utilized over half a century ago, is rapidly becoming an essential tool for enhancing the flow of information within supply chains and improving security in the agri-food industry. Contrary to the perception that RFID is already fully integrated and widely implemented, it has the potential to significantly enhance current supply chain processes. This study aimed to demonstrate the ongoing relevance of RFID technology, particularly in assessing the quality and freshness of fruits. To illustrate the application of RFID technology for quality assessment. The tag, designed and fabricated in this study, features an octagonal geometric shape with a PET substrate, measuring a minimum area of 1.83 cm². The proposed tag operates within a frequency range of 6.7 GHz to 11.8 GHz and can store approximately 127 bits of data. Simulations conducted indicate notable performance enhancements, particularly in its RCS response for evaluating mango quality. Furthermore, the article discusses the fundamental impedance-matching processes involved in the design of a meander line slot microstrip antenna tag. When the impedance of the antenna aligns with that of the integrated circuit (IC) chip, a significant portion of power is delivered to the antenna rather than being reflected back to the source. The article also provides insights into other important RFID IC chips and their characteristic impedances at 866 MHz within RFID systems, describing these chips using similar RC series circuits and considering the impact of resistance on the impedance in the communication output of RFID antennas. In conclusion simulation results are provided which prove that both of the proposed antenna designs exhibit the desired return loss and resonant frequency for UHF RFID systems.

Keywords**:** RFID, Fruit Freshness, Antenna Designs, RCS, Resonant Frequency, Bit Encoding, RFID IC chip, Impedance Matching

1. Introduction

RFID has recently been applied in the agricultural sector to improve quality control of perishable produce which has attracted a lot of interests. In a detailed literature review, [1] explained how RFID transformed the cold chain of perishable produce particularly agricultural produce. This technology is very promising for improving quality control especially of products that are rich in nutrients that degrades with some time. Specifically, [2] investigates the possibility of using RFID technology to track food temperature and identifies improvement areas for the cold chain industry. Such teachings are useful to the food distribution stakeholders to seek ways on how to maximize on the challenges of RFID and how to bring on more of it in order to have quality agricultural products.

RFID technology sustains quality of the foods shipped through the supply chains today. RFID applications for cold chain monitoring associated with the recent advances are the concern of this paper. The work enhances knowledge of how RFID can mitigate problems in the agri-food chain, making it more topical as supply chain management becomes increasingly complex and driven to find new ways of maintaining and enhancing its performance. The rationale for the current research goes hand in hand with the larger aim of addressing the global issue of food waste which is costly to natural, human, and economic capital. The study therefore suggests a waste disposal system that will harness food waste into a resource utility. This is possible through engagement of core actors along the food chain, improvement in quality of data and lastly preventive measures. One goal is to increase consumers' awareness so that they could use efficient measures to return the amount of food waste

In particular this study is centred on the Tommy Atkins mango and aims at advancing the earlier study done by [3]. It looks into the matters of reducing fruit wastage by including an RFID based system that is able to determine shelf life and quality after fruits have been harvested. A new design of octagonal RFID tag is presented [4], made from copper sheet on PET substrate, lowers the size of resonators and optimizes parameters.

Modern RFID technology has been in existence for over fifty years and remains an important enabler of increasing the flow of information and security within supply chains. This has further shown that RFID is underutilized in its capacity towards further improving efficiency, and not as optimally as people believed it to be. Research carried out by [5]. show that its importance cannot be overemphasized especially in testing the freshness and quality of fruits.

This application of the research is demonstrated using an octagonal RFID tag for assessing mango freshness. This compact tag consists of a PET substrate with a size of 13.55mm x 13.55mm, operating at 6.7–11.8 GHz and having storage of 127 bits. Such models corroborate those improvements, particularly with regards its Radar Cross-Section (RCS) counterpart for evaluating quality. Furthermore, a brief analysis of the importance of impedance matching in the design of a meander line slot microstrip antenna tag is presented. The matching of the antenna impedance to that of the RFID IC chip enable maximum power transfer and minimal reflection losses.

2. Methodology

2.1. Design of first tag

The first tag design consists of modified octagonal resonators with seven distinct bits within a compacted size of 1.83 cm². The tag has been designed using CST Microwave Design Studio and printed on 1.575 mm thick polyethylene terephthalate "PET" substrate, with $\epsilon r = 3$ and a loss tangent of 0.002 and is modified as shown in Fig.1. The antenna tag's geometric structure is a sequence of concentric hexagonal rings with reducing side lengths. The outermost octagonal ring has highest dimensions, while successive rings decrease correspondingly in size, as shown by specified measurements. The tag's core is formed by a solid octagon in the structure's centre. An inter-slot gap of 0.2 mm and 0.15 mm is chosen between the first and the fourth resonators and from the fourth to the eighth resonators, respectively, to ensure minimal coupling effects while maintaining a compact tag size. On similar set of substrates proposed tag does not contain any ground plane since the design incorporates a sheet, in Fig.2, is a slot-based resonator that it etched from a square silver sheet having a thickness of 35 µm, as cited in Table I. Each ring and spacing is meticulously constructed for maximum electromagnetic performance, with dimensions and inter-ring spacing crucial for tuning the antenna's resonance frequency. The tag design shows accurate layering of conductive parts designed for electromagnetic performance. The configuration and spacing of the octagonal loops are critical for managing characteristics such resonance frequency and impedance matching, making it ideal for RFID or wireless sensing applications. The outside sheet border adds structural and boundary context to the tag's placement. The tag is excited using linearly polarized electromagnetic waves vertically, as shown in Fig.3, which allows for greater flexibility in tag placement and orientation, making it easier to read tag from various angles. Linear polarization is commonly used in applications where the tag's orientation may vary, such as in supply chain management.

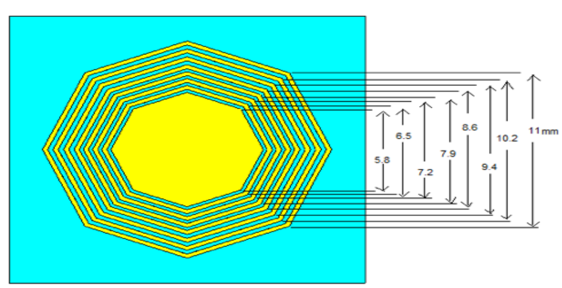

Fig. 1: Octagonal Concentric Antenna Tag Geometry with Dimensional Annotations

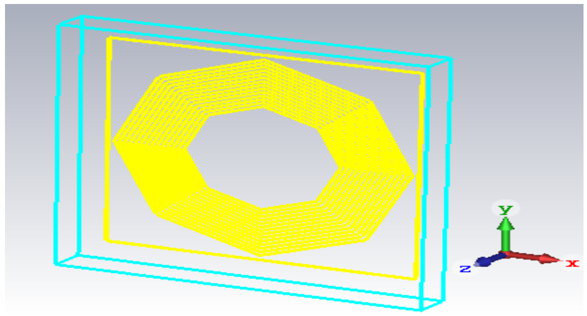

Fig.2: Octagonal Concentric Antenna Tag Design with outer sheet

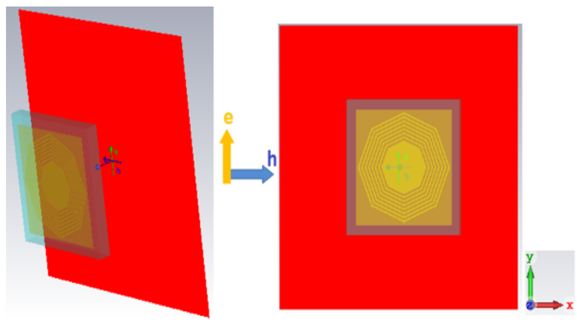

Fig.3: Excitation using a linearly polarized electromagnetic wave

Table 1: Material and Geometric Parameters of First Antenna Tag Design.

Parameters	Values
Substrate	PET
Sub	1.575
ϵ	3
tanδ	0.002
L_{sheet}	11.5
W_{sheet}	11.5
h_{sheet}	0.035
w_{sheet}	0.2
$d_{inner\ ring}$	5.4
$d_{outer\ ring}$	11
Inter-slot gap	0.2

2.2. Design of second tag

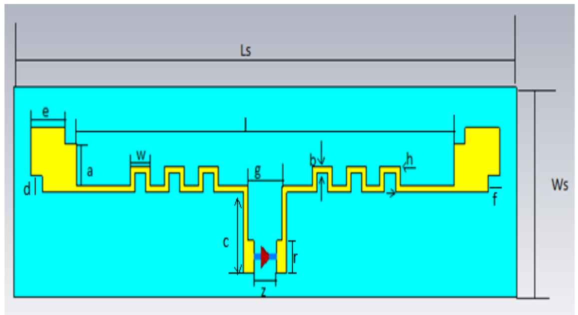

Fig .4: Cross-sectional Layout of a meander line slot microstrip antenna on PET Substrate

The proposed tag antenna geometry with the parameters designed using the PET substrate (εr=3, tan δ=0,002, thickness h=0.98496 mm≈1 mm). By increasing and varying the scale factor, the geometric values are changed.

Table 2: Input Parameters for the design meander line slot microstrip antenna

Parameters	Values
L_s	114
W_s	33
a	6.6
b	1.0
c	12.9
d =f	2.6
e	7.7
g	7.7
h	4.2
l	85.5
r	5.1
w	4.5
z	5.1

2.4. Equations

Impedance matching is the process of eliminating matching losses. In other words, we want to minimize the reflection coefficient, reduce the power reflected from the load the antenna and maximize the power delivered to the antenna. This is one of the fundamental tasks in making an antenna radiate and is therefore one of the most important topics in antenna theory, as shown in Eqs. (1) - (2):

$$R_p = \frac{R_e(Z_c)^2 + Im(Z_c)^2}{R_e(Z_c)} \tag{1}$$

R_p: Resistance of the antenna

$R_e(Z_c)$: Real part of the chip's impedance.

$Im(Z_c)$: Imaginary part of the chip's impedance

$$C_p = \frac{Im(Z_c)}{2\pi f(Im(Z_c)^2 + R_e(Z_c)^2)} \tag{2}$$

C_p: Capacitance of the antenna

$Im(Z_c)$: Imaginary part of the chip impedance.

$R_e(Z_c)$: Real part of the chip impedance.

f: Resonance frequency

by calculating the values of the resistance and capacitance in series from the chip impedance Eq (3) and Eq (4) which:

$$Z_{antenna} = R_p + J X_p \tag{3}$$

$Z_{antenna}$: Antenna impedance
R_p: Resistance's antenna
J: Imaginary unit
X_p: Reactance's antenna

$$Z_{Chip} = R_c - J X_c \tag{4}$$

Z_{Chip}: IC chip impedance
R_c : Resistance's chip.
J: Imaginary unit
X_c: Reactance's IC chip

Therefore, the tag antenna impedance should be nearly meet the conjugate matching with the IC chip and to get a good efficiency using the following Eqs. (5) - (6):

$$R_s = R_e(Z_c) \tag{5}$$

R_s: Series resistance
$R_e(Z_c)$: Real part of the chip impedance

$$C_s = \frac{1}{2\pi f\, Im(Z_c)} \tag{6}$$

C_s : Capacitance for conjugate matching.
f: Resonance frequency
$Im(Z_c)$: Imaginary part of the chip impedance

3. Analysis & Synthesis
3.1. Results per method for the first design

The results of the simulation for the octagonal antenna are operating at its fundamental frequency of 6.76 GHz, as indicated in Fig.5.

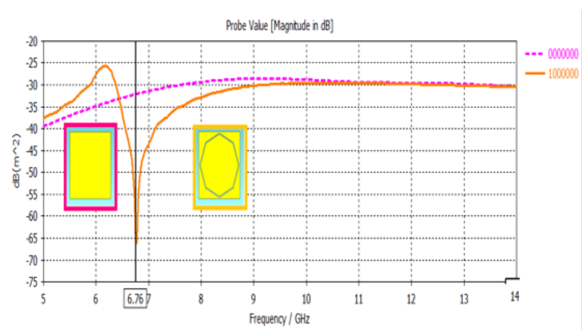

Fig.5: Magnitude response of RCS of one-bit resonator at 6.76 GHz

The surface current distribution of the resonator is depicted in Fig.6, as shown the current distribution on the top and bottom parts of the slot is minimal, indicating a capacitive behaviour. On the other hand, it is relatively maximum on the left and right sides of the octagonal structure, indicating an inductive effect. Overall, the results suggest that the slot orthogonal resonator has a complex impedance that depends on both the inductive and capacitive effects, which can be useful in our application.

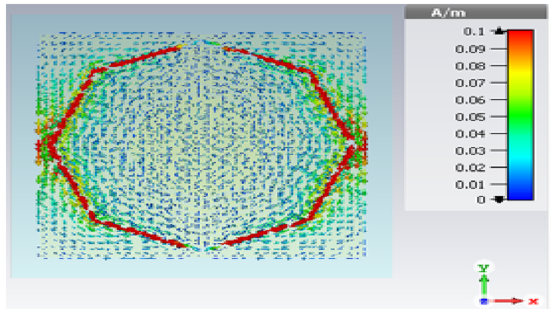

Fig.6: One-bit resonator surface current distribution

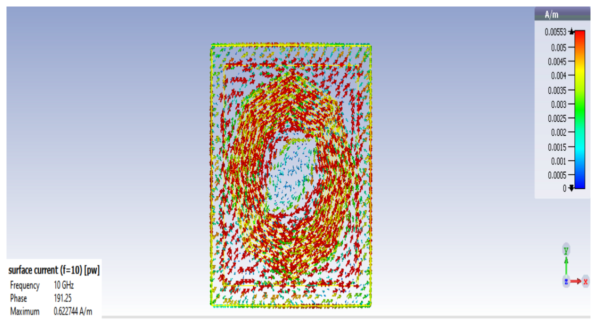

Fig.7. Eight-bit resonators surface current distribution

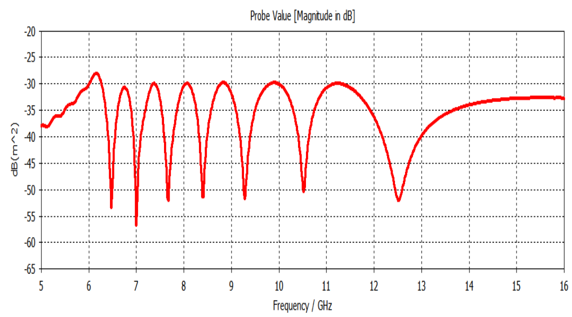

Fig.8: The first tag's RCS result

The computed and measured RCS results for the first tag's electromagnetic performance is demonstrated, where the Radar Cross Section is a measure of how detectable an object or target is by radar. The RCS response of the bit words 00000000, 11111111 is investigated and shown in Fig.8. It is observed that there is a very little shift in the adjacent frequencies after the removal of the slots, due to the mutual coupling between the slot resonators. For different bit combinations 01111111, 10111111, 11011111, 11101111,11110111, 11111011, 111111101, 111111110 are simulated. it's seen a small drift along the frequency axis can be observed for different random sequences when compared with all one's.

3.2. Results per method for the second design

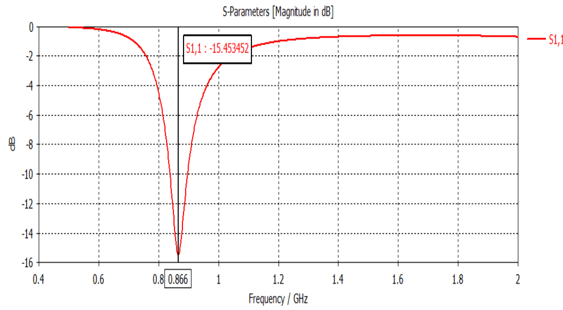

Fig.9: The resonance frequency of a meander line slot microstrip antenna

The results of the simulations conducted to evaluate the antenna's performance are presented in Fig.9 the reflection coefficient S11 at 866 MHz show the characteristics of the antenna.

Table 3: Performance results for the design meander line slot microstrip antenna

Results	Values
f_r(GHz)	0.866
S_{11}(dB)	−15.45
Gain (dB)	1.93
Directivity (dBi)	1.98
Efficiency (%)	97.47

The value of $S_{11} = -15.45\ dB$shows that a significant portion of the input power is transmitted into the antenna with minimal reflection. Typically, an $S_{11} = -10dB$ is considered acceptable for antenna performance, and here the S_{11} below is even better, indicating good impedance matching. The antenna's gain is moderate with a value of 1.93 dB which is suitable for compact design. And a high efficiency equal to 97.47%.

About the polarization of the octagonal antenna design the plane wave has circular polarization (LCP), meaning the electric field vector rotates in a circle as the wave propagates, in a left-handed orientation. The plane wave propagates along the z-direction, as specified by the wave normal vector (0,0,1). The electric field vector is defined as (1,0,0), indicating its initial orientation along the x-axis. The reflection frequency is shown as 6.76.

the polarization performance of the second design across a range of frequencies for an all "1's" sequence, showed a uniformity in magnitude across polarizations and frequencies, except for these dips, might suggest good polarization stability, where was concluded after multiple plotted different polarization angles that the proposed tag design is polarization insensitive for ϕ=10 °, making it valuable in practical utilization.

3.3. Impedance match for meander line slot microstrip antenna tag

Table 4: Comparative analysis of parameters for five RFID tags model

RFID Tag Model	RF Frequency (MHz)	Impedance $Z_{antenna}$ Z_{Chip} (Ω)	R_s (Ω)	C_s (pF)
Alien Higgs-4	860~960	27±j205	27	0.89
NXP G2XM		24±j206	22	
Impinj Monza 4		13±j151	13	1.21
		17±j105	17	1.73

Murata LXMS31ACNA				
Impinj Monza R6		13±j126	13	1.45

Several RFID tags model simulations on the antenna that use the UHF frequency band have been chosen; the most popular ones are shown in table 4. The antenna was used to replicate a range of RFID tag models that operate in the UHF frequency spectrum; Table 4 lists the most popular models. The one with the highest resistance among these was Alien Higgs-4 $R_S = 27\Omega$, which could lead to marginally greater power losses in contrast to other models. On the other hand, Murata LXMS31ACNA showed the highest capacitance $C_S = 1.735\ pF$, which probably affects its resonant frequency behaviour and makes it especially appropriate for lower-frequency UHF band applications. These variations show how efficiency, impedance matching, and frequency response characteristics are traded off in the various tag models.

Table 5: performance characteristics of various RFID tag models

RFID Tag Model	Frequency Range (MHz)	S_{11} (dB)	Bandwidth (MHz)
Alien Higgs-4	860- 861	-26.10	83
NXP G2XM		-21.56	84
Impinj Monza 4		-34.65	78
Murata LXMS31ACNA		-31.17	82
Impinj Monza R6		-34.65	78

The lowest resonant frequencies are 860 MHz for NXP G2XM and Alien Higgs-4, and 861 MHz for other tags Impinj Monza 4 and Impinj Monza R6 have the best reflection coefficients -34.65 dB, suggesting good impedance matching and minimal power reflection. NXP G2XM has the highest is least favorable S11 value, -21.56 dB.

4. Findings and discussion

Table 5: [1]Octagonal concentric antenna design, performance, and practicality; [2]Impedance matching for meandered slot microstrip antennas with IC chips;[3]Discussion of their optimization.

<table>
<tr><td>Design antennas</td><td colspan="5"></td></tr>
<tr><td rowspan="3">[1]Octagonal Concentric</td><td colspan="2">[1]Design Innovations</td><td colspan="2">[1]Performance and Practicality</td><td>[3]Optimization Goals</td></tr>
<tr><td>Bit capacity</td><td>f_r(GHz)</td><td>Flexibility</td><td>Material and Fabrication</td><td rowspan="2">8 bits in 13.5 cm^2 on PET substrate improve RCS response and read range</td></tr>
<tr><td>2^3</td><td>6-11</td><td>2x3 unit element (curvature radius 10~100 mm)</td><td>PET</td></tr>
<tr><td rowspan="2">[2]Meander line slot microstrip</td><td colspan="2">[2]Best Performance for</td><td colspan="2">Impinj Monza 4
Impinj Monza R6</td><td rowspan="2">Creating versatile, high-efficiency</td></tr>
<tr><td colspan="2">[2]Widest Bandwidth for</td><td colspan="2">NXP G2XM</td></tr>
</table>

	[2]Balanced Performance for	Alien Higgs-4 Murata LXMS31ACNA	Creating versatile, high-efficiency antennas and advancing broadband solutions suitable for our application

4. Conclusion

The consumption of electromagnetic food such as vegetables and fruits provide energy to the human body, and to trace the quality of these fruits and vegetables, we can use the RFID system to detect their contamination. In this article, we developed two types of tags: Octagonal Concentric and Meander Line Slot Antennas, where we analysed their characteristics using CST Studio, as well as the impedance match of the second antenna to have more efficient and effective tag antennas.

Octagonal Concentric Antenna: This design achieved an operating frequency between 6.7 GHz and 11.8 GHz. The tag uses an 8-bit encoding system. It demonstrated an improved Radar Cross Section (RCS) response and read range. The simulation results showed that the octagonal antenna operates at a fundamental frequency of 6.76 GHz. The current distribution indicates a complex impedance with both inductive and capacitive effects.

The Meander Line Slot Microstrip Antenna, operating at 866 MHz, matches RFID IC chips with a reflection coefficient of -15.45 dB, moderate gain of 1.93 dB, and high efficiency of 97.47%. Simulations show that both designs have the desired return loss and resonant frequency for UHF RFID systems. To this end, this research article provide insight into a future where technology can reduce food waste, enhance supply chain efficiency, and ensure the availability of perfectly ripe mangoes for everybody.

References

[1] B. M. Sedghy, "How RFID Transformed the Cold Chain of Perishable Produce, Particularly Agricultural Produce," [Online]. Available: https://www.example-link.com. Accessed: Nov. 16, 2024.

[2] A. Ali, C. Smartt, E. Lester, O. Williams, and S. Greedy, "High capacity chipless RFID tags for biomass tracking application," International Journal of Microwave and Wireless Technologies, vol. 15, no. 5, pp. 742–752, 2023.

[3] C. B. Hattab, S. Naoui, and L. Latarch, "Monitoring freshness of tommy mango fruit with an RFID tag," in Microwave Mediterranean Symposium (MMS), Pizzo Calabro, Italy, 2022, pp. 1–6.

[4] D. Betancourt, K. Haase, A. Hübler, and F. Ellinger, "Bending and Folding Effect Study of Flexible Fully Printed and Late-Stage Codified Octagonal Chipless RFID Tags," in IEEE Transactions on Antennas and Propagation, vol. 64, no. 7, pp. 2815-2823, July 2016.

[5] C. Xu and D. Zhao, "Optimal Decisions for Adoption of Item-Level RFID in a Retail Supply Chain with Inventory Shrinkage under CVaR Criterion," Mathematical Problems in Engineering, vol. 2016, Article ID 7834751, 2016, doi: 10.1155/2016/7834751.